Comparative Dissolution Behaviors of Recycled Cement Paste and Lime in EAF Slag under Static Conditions

M. Yang[1], Z. Yan[2] and Z. Li[3]

1. Research Fellow, Advanced Steel research Centre WMG, University of Warwick. Coventry, UK, CV4 7AL. Email: Mingrui.yang@warwick.ac.uk
2. Research Fellow, Advanced Steel research Centre WMG, University of Warwick. Coventry, UK, CV4 7AL. Email: Zhiming.yan@warwick.ac.uk
3. Professor, Advanced Steel research Centre WMG, University of Warwick. Coventry, UK, CV4 7AL. Email: Z.li.19@warwick.ac.uk

Keywords: EAF slag, Recycled cement paste, dissolution, lime

ABSTRACT

Recycled cement paste (RCP) is a kind of CaO-rich recourse, which is separated and recycled from waste concrete. Due to its chemical composition, RCP could partially replace lime as a flux and be loaded into EAF steel making process. Rapid RCP assimilation and liquid slag formation have significant effects on EAF steel making process. In this study, the dissolution behaviours of RCP and lime at temperatures of 1400 °C to 1500 °C were investigated using static dissolution experiment. The dissolution rate, interfacial microstructure, as well as dissolution mechanisms were discussed. It was found that the dissolution rate of RCP was much higher than that of lime. RCP could be completely dissolved into slag in 60 seconds at 1500 °C. The dissolution rate of lime was in range of 3.9×10^{-4} g/(cm^2·s) to 2.6×10^{-3} g/(cm^2·s), while that for RCP was in range of 1.5×10^{-3} g/(cm^2·s) to 4.9×10^{-3} g/(cm^2·s). As for lime dissolution, a dense layer of dicalcium silicate (C_2S) generated at the dissolution interface, and the diffusion of Ca^{2+} in C_2S layer was the limited step for lime dissolution. Some of calcium ferrite could be observed at the interface between lime and C_2S layer. As for the RCP dissolution, there is no obvious product layer of C_2S formed at the dissolution interface, Fe^{2+} continuously diffused into RCP layer during the dissolution, and small amount of FeO·MgO solid solution generated and gathered at the dissolution interface. The dissolution rate of RCP in EAF slag was quite higher than that of lime, partially add RCP as flux in EAF could accelerate the slag formation process.

INTRODUCTION

Recycled cement paste (RCP), a CaO-rich resource obtained through the separation and recycling from waste concrete and cement (Silva et al., 2022; Bordya et al., 2017), could partially replace lime as a flux in the EAF steelmaking process for resource utilization (Wang et al., 2018; Zhutovsky et al., 2021). In the EAF steelmaking process, rapid slag formation plays a crucial role in refining reactions, resulting in a shortened refining duration and energy savings, and the slag formation is heavily influenced by the dissolution of flux into the slag ((Wang et al., 2018; Zhutovsky et al., 2021).

In last decades, many experiments (Lesiak et al., 2022; Amini et al., 2007; Martinsson et al., 2018; Deng et al., 2012; Li et al., 2014; Fruehan et al., 2013; Kitamura et al., 2017) have been carried out to investigate the dissolution behaviors of solid oxides in steel slag. Lesiak et al. (Lesiak et al., 2022) investigated the effects of calcination condition of dolomite-based materials dissolution in EAF slag, found that the dissolution amount decreases with deceasing of porosity. Fruehan et al. (Fruehan et al., 2013) studied the dissolution of magnesite and dolomite in EAF slag using both the dipping test and rotating cylinder test, found that during the dissolution of dolomite, CaO dissolved away first, and then the MgO particles entered the solution. The dissolution of lime in steel slag is a very common topic for steel making. The influence factors for dissolution could be summarized as: 1) chemical composition of solid and liquid, 2) temperature, 3) particle size, and 4) forced convection. Based on the experimental techniques and influencing factor, these dissolution experiments could be divided into five types: 1) under static conditions; 2) rotating rod/disc method; 3) under forced convection; 4) direct observation and 5) sampling from industry, and these were briefly reviewed by Li Z. et al. (Li et al., 2022).

Based on the dissolution mechanism, the dissolution could be divided into a) direct dissolution and b) indirect dissolution. Direct dissolution, where only physical diffusion occurs without involving chemical reactions, is exemplified in processes such as the dissolution of Al_2O_3 (Yu et al., 2016; Yang et al., 2018) and SiO_2 (Yu et al., 2015; Xiang et al., 2014) into $CaO-Fe_2O_3$-based slag, dissolution of Al_2O_3 into $CaO-Al_2O_3-SiO_2$ slag (Cho et al., 2004). Dissolution of solid oxide into slag may involve the formation of an intermediate reaction product, and this type of dissolution is called as indirect dissolution. Sandhage et al. (Sandhage et al., 1988) observed that spinal ($MgAl_2O_4$) formed at the $Al_2O_3/CaO-SiO_2-MgO-Al_2O_3$ interface. Yu et al. (Yu et al., 2015) and Yang et al. (Yang et al., 2018) found the $MgFe_2O_4$ and $CaTiO_3$ produced at the $MgO/CaO-Fe_2O_3$ and $TiO_2/CaO-Fe_2O_3$ interface. While product layer of $CaAl_4O_7$ could be found near the sapphire/$CaO-SiO_2-Al_2O_3$ interface, reported by Oishi et al. (Oishi et al., 1965). As for the lime dissolution into $CaO-SiO_2$-FeO based slag (generally BOS slag and EAF slag), it has been confirmed that the formation of C_2S phase during the dissolution process, and the C_2S crystal distribution depends on the experimental conditions. The reaction of CaO and SiO_2 to produce C_2S is considered inevitable in these conditions. Typically, the C_2S phase demonstrates high thermodynamic stability in $CaO-SiO_2-MgO-Al_2O_3$-FeOx slag systems, particularly under basicity ranging from 1.5 to 3.0 at high temperatures.

RCP is a CaO-rich resource that can fully or partially replace lime as a flux in EAF steelmaking. The dissolution process, dissolution mechanism and dissolution rate of RCP also play a crucial role in EAF slag formation, but these have not been fully understood or reported yet. This study aims to explore the dissolution behaviors of RCP and lime (for comparison) in simulated EAF slag at 1400 °C and 1500 °C under static conditions. The dissolution process, dissolution interfacial microstructure, and dissolution mechanisms were thoroughly discussed.

EXPERIMENTAL

Materials preparation

The recycled cement paste (RCP) is made by commercial Portland cement with water at a water to cement mass ratio of 0.6. It was then cured at room temperature for one month in sealed condition to avoid evaporation. After curing, these cement paste bricks were heated up around 450 °C to 500 °C in a muffle furnace to produce RCP. The chemical and phase compositions of RCP were examined by XRF (PANalytical Epsilon 3) and XRD (Panalytical Empyrean, Co target). The RCP was of the following composition: 68.093 pct. CaO, 19.455 pct. SiO_2, 4.864 pct. Al_2O_3, 0.737 pct. MgO, 3.613 pct. Fe_2O_3, 0.486 pct. K_2O, 0.120 pct. Na_2O and 0.250 pct. TiO_2. The XRD result of RCP is shown in **Figure 1**. It can be seen that the phase composition of RCP was mainly composed of dicalcium silicate (C_2S), CaO, and small amount of C_3S, SiO_2 and $Ca(OH)_2$. During the heating process, there were dehydration reactions for calcium silicate hydrate (C-S-H) phase to produce C_3S (tricalcium silicate) and C_2S. Then the C_3S phase would decompose into C_2S and CaO because C_3S is not thermodynamic stable at the roasting temperature. Some of $Ca(OH)_2$ were detected due to the moisture absorb of CaO.

The slag used was synthesized to simulate the initial liquid EAF slag before steel refining. The investigation of RCP and lime dissolution in slag has been carried out with a synthesized EAF steelmaking slag of the following chemical composition: 40 pct. of CaO, 30 pct. of SiO_2, 20 pct. of FeO, 6 pct. of MgO and 4 pct. of Al_2O_3. The chemical reagents of CaO, SiO_2, MgO, Al_2O_3 and FeO in purity of 99.5 wt. pct. (Alfa Aesar) were used to prepare the slag samples and CaO tablet. Homogeneously mixed the chemical regents powder using a ball milling at ratio of grinding ball mass to material mass of 5:1 for 30 mins. Then used a cylinder mold to press them into tablets and pre-melted the slag tablet in a sealed furnace at 1500 °C in Argon atmosphere for 30 min. To minimize the influence of solid porosity on dissolution behaviors, the sintered dense solid tablets of CaO and RCP were prepared for dissolution experiments. The CaO and RCP powders were load into a cylinder mold with diameter of 5mm under 1 ton pressure for 1min, then roasted the solid sample of CaO and RCP in a muffle furnace in air for 10 hours at 1400 °C and 1000 °C, respectively.

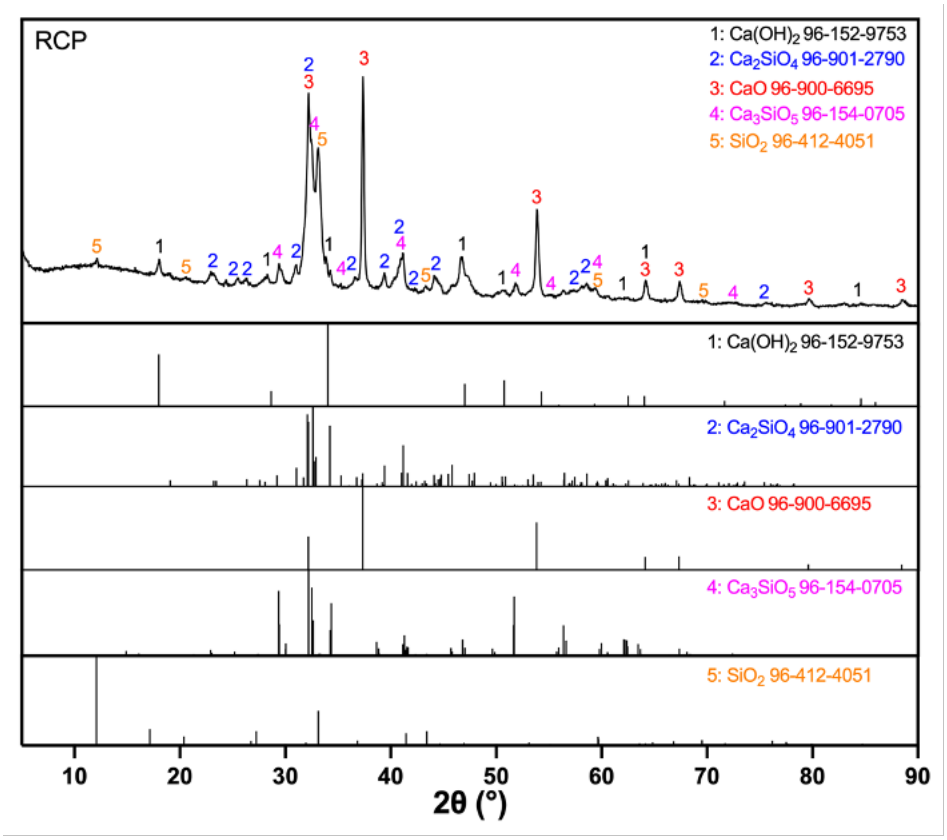

FIG 1 – XRD patterns of recycled cement paste and standard components

Dissolution experiment

The dissolution experiments were carried out in a confocal laser scanning microscope furnace at 1400 °C and 1500 °C in Argon, the schematic diagram for device is shown in **Figure 2**. The chamber is ellipsoid in shape, with the heating element and sample holder positioned at the upper and lower focal points of the ellipsoid. The heating principle involves the reflection and focusing of thermal radiation through the gold coating on the chamber. The dissolution times were 30s, 60s, 90s, and 120s. The heating and cooling rates were set as quickly as possible at 400 K/min and -1200 K/min, respectively, to minimize dissolution time errors. Zero dissolution time was defined as the moment when samples reached the desired temperature. The experimental conditions, geometry size of solid samples, etc., are summarized in **Table 1**. The samples labelled from L1 to L8 represent lime dissolution samples, while those labelled from R1 to R8 represent RCP dissolution samples. After dissolution, the samples with crucibles were embedded in resin, subsequently cut, and polished along the cross-section. The thickness of solid parts after dissolution was measured using a digital optical microscope (OM, Keyence VHX7000), while the microstructure and element distribution of the dissolution interface were examined using a scanning electron microscope (SEM, Zeiss, Sigma) equipped with energy dispersive X-ray spectroscopy (Oxford, Ultim Extreme).

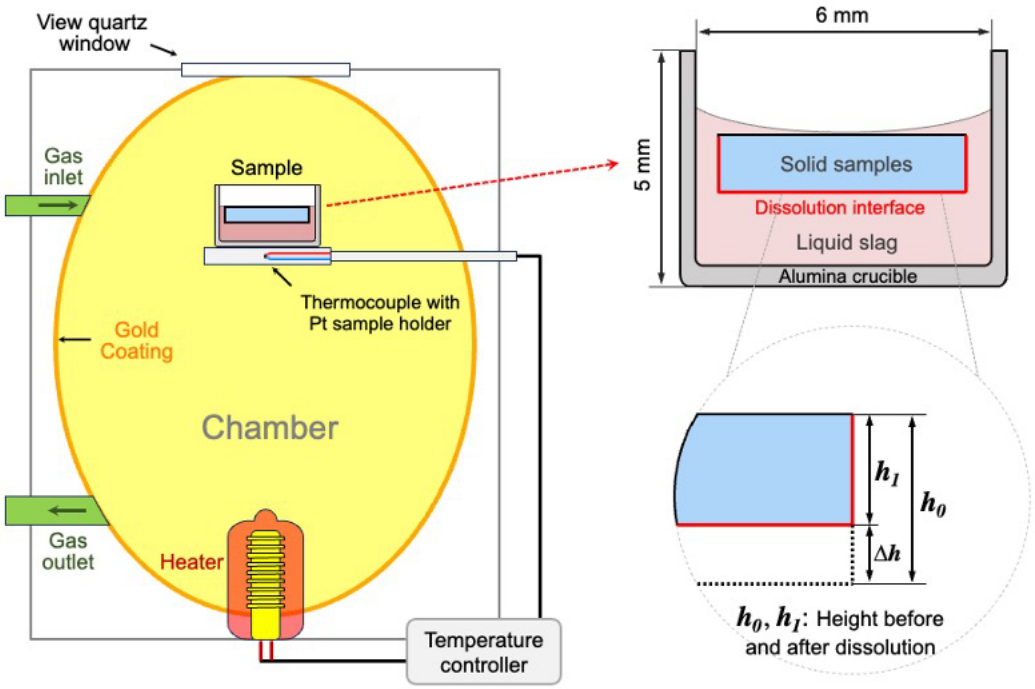

FIG 2 – Schematic of confocal laser furnace and present dissolution experiments.

RESULTS AND DISCUSSIONS

Dissolution behaviors

The density of RCP ranges from 2.43 g/cm^3 to 2.51 g/cm^3, while that of lime ranges from 2.63 g/m^3 to 2.66 g/m^3. The density of liquid slag is 2.83 g/cm^3. During the dissolution process, the solid samples of RCP and lime tend to float in the liquid slag due to their lower densities compared to that of the liquid slag. The liquid slag exhibits good wettability on both the solid samples and the Al_2O_3 crucible. It can be observed in **Figure 3** that the solid samples are continuously and gradually wetted by the liquid slag. Assuming that the shape of the solid parts in slag after dissolution still remains cylindrical, the height of the solid sample after dissolution was measured using an optical microscope. The dissolution of the solid sample in the liquid slag primarily occurred through the bottom and sides of the cylinder. Consequently, the decrease in sample height (Δh) and the decrease in sample radius (Δr) can be considered as the same value, $\Delta h = \Delta r$. The volume, weight, weight loss, and weight loss fraction after dissolution can also be calculated, and the weight loss fraction for solid samples after dissolution are summarized in **Table 1** and in **Figure 4**. The experimental results indicate that the dissolution of RCP at 1500 °C slowed down and eventually stopped at 60s. In samples R6, R7, and R8, no original solid RCP parts could be observed, indicating that RCP had completely dissolved into the slag in these samples. Based on the weight loss of samples, the dissolution rate of RCP could be calculated as 13.73×10^{-5} m/s and 29.05×10^{-5} m/s at 1400 °C and 1500 °C, while that of lime are 3.12×10^{-5} m/s and 8.42×10^{-5} m/s at 1400 °C and 1500 °C.

TABLE 1 – Dissolution conditions and measured parameters of samples

Samples	Temperature	Dissolution Time (s)	Weight loss fraction
L1	1400	30	0.1067
L2	1400	60	0.1673
L3	1400	90	0.1967
L4	1400	120	0.2285
L5	1500	30	0.2647
L6	1500	60	0.3917
L7	1500	90	0.4409

L8	1500	120	0.4784
R1	1400	30	0.3536
R2	1400	60	0.5460
R3	1400	90	0.6244
R4	1400	120	0.6800
R5	1500	30	0.7421
R6	1500	60	1
R7	1500	90	1
R8	1500	120	1

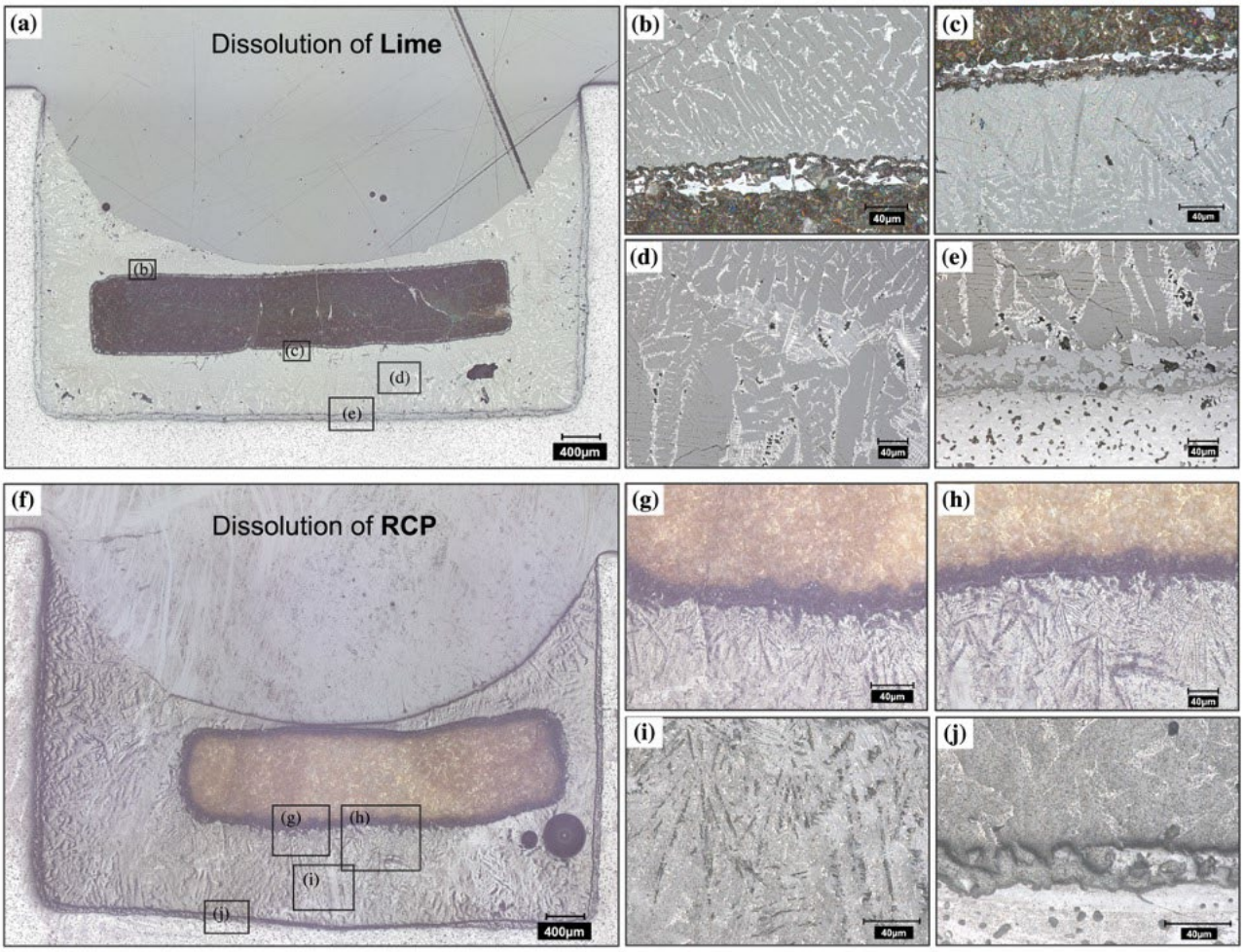

FIG 3 – Optical images for cross section of samples, (a) to (e): L2 (lime, 1400 °C, 60s); (f) to (j) R2 (RCP, 1400 °C, 60s).

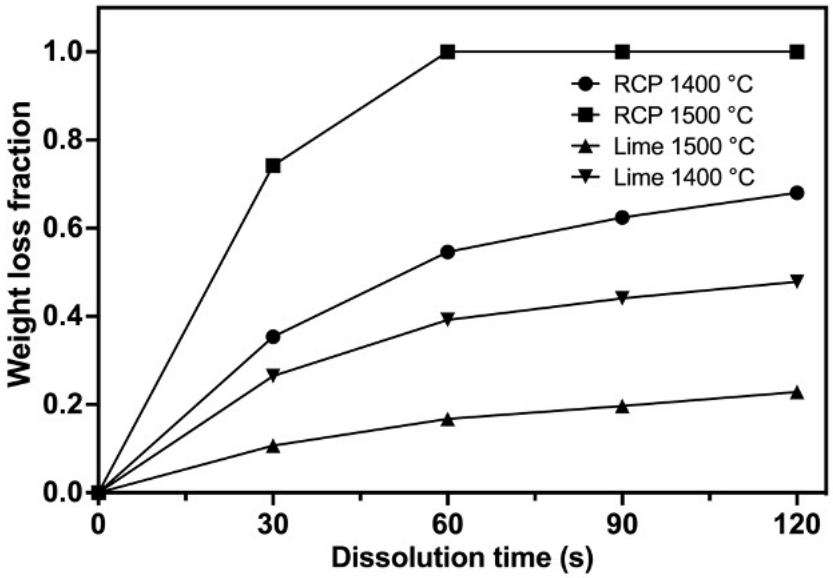

FIG 4 – Dissolution weight loss fraction of RCP and lime in different temperature and dissolution time

Interfacial microstructure

Figure 5 displays the scanning electron microscope (SEM) image and energy-dispersive X-ray spectroscopy (EDS) results illustrating the interfacial microstructure of lime dissolution in slag. The presence of the Fe element was detected in the lime layer, indicating that a small amount of slag had penetrated into the lime layer during the dissolution process. Results reveals that the bright area is primarily composed of Ca, Fe, and O, suggesting that this phase corresponds to a calcium ferrite-based slag phase. From the EDS mapping results of Ca and Si, it can be seen that a significant dense product layer of C_2S, with a thickness of approximately 20 μm, is clearly visible at the forefront of the dissolution interface layer. The observed interfacial microstructure during the dissolution of lime into EAF slag aligns with previously reported findings (Lesiak et al., 2022; Amini et al., 2007; Martinsson et al., 2018; Deng et al., 2012; Li et al., 2014). Those studies also noted the accumulation of a C_2S product layer at the dissolution interface of lime into steel slag (CaO-SiO_2-FeO based slag). Deng *et al*. (Deng et al., 2012) investigated the dissolution of lime in steel slag (CaO-SiO_2-FeO) under forced convection and concluded that the removal of the C_2S dense product layer by liquid forced mobility could accelerate the lime dissolution process. They also identified some tricalcium silicate (C_3S) crystals generated at the dissolution interface and within the lime layer. The dissolution of lime into slag at high temperatures depends on dissolution of dense C_2S layer into liquid slag. In the liquid slag layer, massive crystals of C_2S and a small amount of fine iron oxide crystals precipitated along with the C_2S crystals. No tricalcium silicate (C_3S) phases were found at the dissolution interface. The main reaction for C_3S formation is $C_2S+CaO=C_3S$. The formation of C_3S requires certain conditions, such as a specific temperature (>1300 °C) and sufficient reaction time. However, the maximum dissolution duration in the present experiments is 120 seconds, and the reaction time is insufficient for the formation of C_3S.

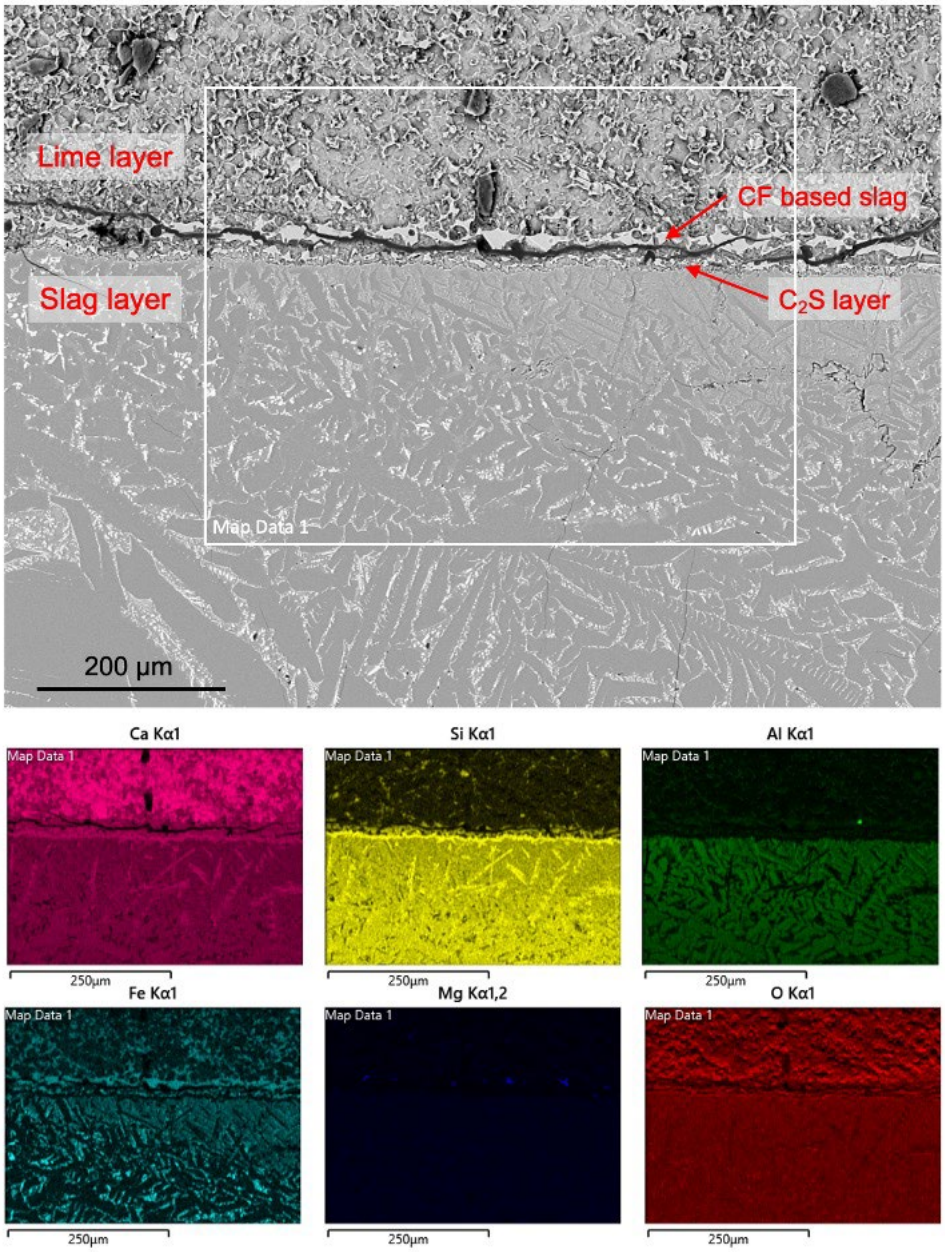

FIG 5 – SEM image and EDS results for dissolution interface of sample L2 (Lime, 1400 °C, 60s)

The SEM images and EDS results depicting the interfacial microstructure of RCP dissolution are shown in **Figure 6**. In comparison with the dissolution of lime, no dense product layer of C_2S could be observed in the samples, and some dendritic C_2S crystals can be found in the slag. EDS results show that some of FeO_x could be detected in RCP layer, indicating that some of Fe ions diffused into the solid RCP layer during dissolution process. The thickness of the sample-slag interlayer is approximately 100μm. The Al_2O_3 content in the sample-slag interlayer is higher than that in the slag bulk, indicating that AlO_4^{5-} diffuses in the slag bulk and accumulates in the interlayer. Some of massive C_2S crystals and fine FeO_x could be detected in residual slag. As mentioned before, the phase in RCP is mainly composed of C_3S, C_2S, CaO and SiO_2, these phases could directly dissolve into EAF slag. The content of CaO in RCP is too low to produce a dense layer of C_2S. But in dissolution of lime, C_2S would be produced, and it is hard to remove under static conditions. The dissolution process of C_2S is the limiting step in lime dissolution; this is the main reason for the dissolution of RCP is faster than that of lime.

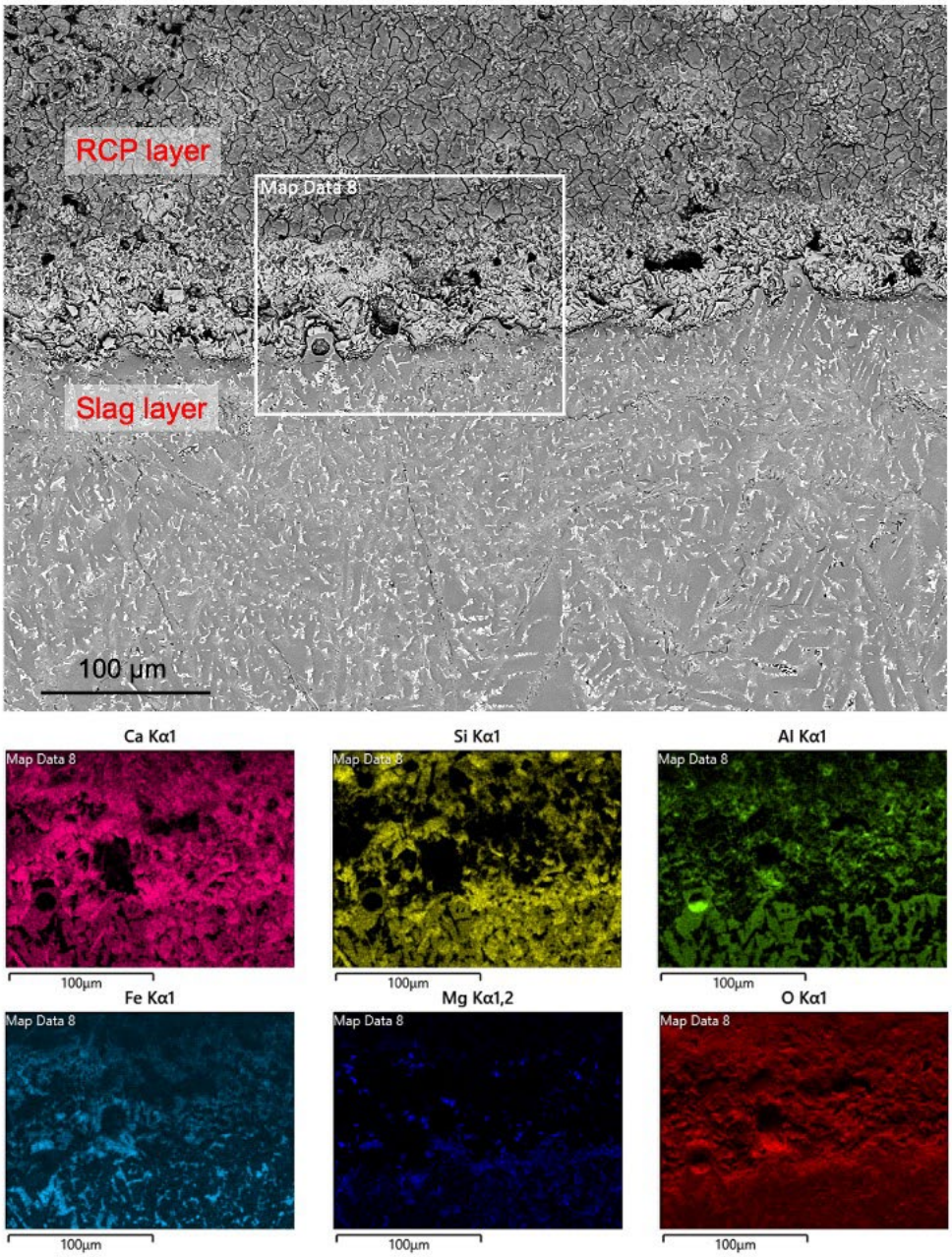

FIG 6 – SEM image and EDS results for dissolution interface of sample R2 (RCP, 1400 °C, 60s)

CONCLUSIONS

The dissolution behaviors of recycled cement paste (RCP) and lime at temperatures of 1400 °C and 1500 °C were investigated under static conditions. The RCP could be completely dissolved into slag in 60 seconds at 1500 °C, and the dissolution rate of RCP is much higher than that of lime. The dissolution rate of lime was in range of 3.9×10^{-4} g/(cm^2·s) to 2.6×10^{-3} g/(cm^2·s), while that for RCP was in range of 1.5×10^{-3} g/(cm^2·s) to 4.9×10^{-3} g/(cm^2·s). A dense product layer of dicalcium silicate generated at the dissolution interface, with the dissolution of this dense C_2S layer identified as the limiting step for lime dissolution. Calcium ferrite could be observed at the interface between lime and C_2S layer. In the dissolution of RCP, there is no apparent product layer of C_2S formed at the dissolution interface. Fe^{2+} continuously diffuses into the RCP layer during the dissolution process. Generally, the dissolution rate of RCP in EAF slag was quite higher than that of lime, partially add RCP as flux in EAF could accelerate the liquid slag formation process in EAF.

ACKNOWLEDGEMENTS

The authors gratefully acknowledge the financial support from EPSRC Grant No. EP/W026104/1.

REFERENCES

Amini S., Brungs M., Ostrovski O. (2007). Dissolution of Dense Lime in Molten Slags under Static Conditions. ISIJ International, 47(1), 32-37.

Bordya A., Younsib A., Aggoun S., Fiorioa B. (2017). Cement substitution by a recycled cement paste fine: Role of the residual anhydrous clinker. Construction and Building Materials, 132, 1-8.

Cho W., Fan P. (2004). Diffusional Dissolution of Alumina in Various Steelmaking Slags. ISIJ International, 44, 229-234.

Deng T., Du S. (2012). Study of Lime Dissolution Under Forced Convection. Metall. Mater. Trans. B, 43B, 678-86.

Fruehan R., Li Y., Brabie L. (2003). Dissolution of magnesite and dolomite in simulated EAF slags. Isstech-conference Proceedings. Iron And Steel Society.

Kenneth H. Sandhage, Gregory J. Yurek. (1988). Indirect Dissolution of Sapphire into Silicate Melts. J. Am. Ceram. Soc., 71(6), pp. 478-89.

Kitamura S. (2017). Dissolution Behavior of Lime into Steelmaking Slag. ISIJ Int., 57(10), 1670-76.

Lesiak S., Cheremisina E., Rieger J., Schenk J., Firsbach F., Johnson W., Chopin T., Nispel M. (2022). Calcination Condition of Dolomite-Based Materials Influencing Static Dissolution in Synthetic Electric Arc Furnace Slag. Steel Res. Int.. 93, 2100675.

Li Z., Whitwood M., Millman S., Boggelen J. (2014). Dissolution of lime in BOS slag: from laboratory experiment to industrial converter. Ironmaking & Steelmaking, 4, 112-21.

Li Z., Li J., Spooner S., Seetharaman S. (2022). Basic Oxygen Steelmaking Slag: Formation, Reaction, and Energy and Material Recovery. Steel Res. Int., 93, 2100167.

Martinsson J., Glaser B., Du S. (2018). Lime Dissolution in Foaming BOF Slag. Metall. Mater. Trans. B, 48B, pp. 3164-70.

Oishi Y., Y., Cooper A. J R, Kingery W. (1965). Dissolution in ceramic systems: III, boundary layer concentration gradients. Journal of the American Ceramic Society, 48(2), 88-95.

Silva A., Nogueira R., Bogas A., Abrantes J., Wawrzynczak D., Sciubidło A., I. M. Kucęba. (2022). Valorisation of Recycled Cement Paste: Feasibility of a Short-Duration Carbonation Process. Materials, 15(17), 6001.

Wang J., Mu M., Liu Y. (2018). Recycled cement. Construction and Building Materials, 190, 1124-32.

Xiang S., Lv X., Yu B., Xu J., Yin J. (2014). The dissolution kinetics of Al_2O_3 into molten CaO-Al_2O_3-Fe_2O_3 slag. Metall. Mater. Trans. B, vol.45B, 2106-17.

Yu B., Lv W., Xiang S., Bai C., Yin J. (2015). Wetting behavior of calcium ferrite melts on sintered MgO. ISIJ International, 55(8), 1558-1564.

Yu B., Lv W., Xiang S., Bai C., Yin J. (2015). Wetting behavior of Al_2O_3 substrate by calcium ferrite series melts. ISIJ International, 55(3), 483-90.

Yu B., Lv W., Xiang S., Xu J. (2016). Dissolution Kinetics of SiO_2 into CaO-Fe_2O_3-SiO_2 Slag. Metall. Mater. Trans. B, 2016, 47B, 2063-73.

Yang M., Lv X., Wei R., Xu J., Bai C. (2018). Wetting behavior of calcium ferrite slags on cristobalite substrates. Metall. Mater. Trans. B, 49B, pp. 1331-45.

Yang M., Lv X., Wei R., Bai C. (2018). Wetting behavior of TiO_2 by calcium ferrite slag at 1523 K. Metall. Mater. Trans. B, 49B, 2667-80.

Zhutovsky S., Shishkin A. (2021). Recycling of hydrated Portland cement paste into new clinker. Construction and Building Materials, 280, 122510.